

Alendronate Affects Calcium Dynamics in Cardiomyocytes

Naomi Kemeny

Faculty of Graduate Studies

Faculty of Dentistry

McGill University, Montreal

February 16, 2009

A thesis submitted to

McGill University

in partial fulfillment of the requirements
of the degree of Master of Sciences (M.Sc.)
in the Faculty of Dentistry

© Naomi Kemeny 2009

TABLE OF CONTENTS

LIST OF FIGURES	2
ABBREVIATIONS	3
ABSTRACT	4
RÉSUMÉ	5
ACKNOWLEDGEMENTS	6
CONTRIBUTIONS	7
CHAPTER I – LITERATURE REVIEW	8
INTRODUCTION	8
1.1 BISPHOSPHONATES	9
1.1.1 <i>General Overview</i>	<i>9</i>
1.1.2 <i>Bisphosphonate Structure</i>	<i>10</i>
1.1.3 <i>Simple Bisphosphonates</i>	<i>10</i>
1.1.4 <i>Nitrogen Containing Bisphosphonates</i>	<i>11</i>
1.1.5 <i>Side Effects</i>	<i>11</i>
1.2 HEART PHYSIOLOGY AND CALCIUM	12
1.2.1 <i>Structure of The Heart</i>	<i>12</i>
1.2.2 <i>Electrical Activity in The Heart</i>	<i>13</i>
1.2.3 <i>Calcium</i>	<i>14</i>
1.2.4 <i>Important Regulators of Calcium Dynamics in Cardiomyocytes</i>	<i>15</i>
1.2.5 <i>Serca</i>	<i>16</i>
1.2.6 <i>Calsequestrin</i>	<i>16</i>
1.2.7 <i>Calreticulin</i>	<i>17</i>
1.2.8 <i>Caffeine as a Stimulus</i>	<i>17</i>
1.2.9 <i>Atrial and Ventricular Cardiomyocytes</i>	<i>18</i>
1.3 ATRIAL FIBRILLATION	19
1.4 OBJECTIVE AND RATIONALE	20
CHAPTER II – MATERIALS AND METHODS	21
2.1 REAGENTS	21
2.2 CELL CULTURE	21
2.3 ALENDRONATE TREATMENTS	22
2.4 PROTEIN ISOLATION AND IMMUNOBLOT ANALYSIS	23
2.5 FLUORESCENCE MEASUREMENT OF CYTOSOLIC FREE Ca^{2+} CONCENTRATION ..	24
2.6 SPECTRAL ANALYSIS OF CALCIUM OSCILLATIONS	25
2.7 STATISTICAL ANALYSIS	26
CHAPTER III RESULTS	27
3.1 EFFECT OF ALENDRONATE ON FARNESYLATION/GERANYLATION IN HL-1 ATRIAL CARDIOMYOCYTES	27

3.2 EFFECT OF ALENDRONATE ON CALCIUM DYNAMICS IN ATRIAL CARDIOMYOCYTES	29
3.3 SHORT-TERM EFFECT OF ALENDRONATE ON CAFFEINE-INDUCED CALCIUM DYNAMICS IN ATRIAL CARDIOMYOCYTES	32
3.4 LONG-TERM EFFECT OF ALENDRONATE ON CAFFEINE-INDUCED CALCIUM DYNAMICS IN ATRIAL CARDIOMYOCYTES	35
3.5 LONG-TERM EFFECT OF ALENDRONATE ON VENTRICULAR CARDIOMYOCYTES ..	40
CHAPTER IV –CONCLUSION AND DISCUSSION	45
REFERENCES	51
RESEARCH COMPLIANCE CERTIFICATES.....	54

LIST OF FIGURES

CHAPTER 2 - Results

- Figure 2.1 Effect of ALN on protein farnesylation and geranylation in HL-1 atrial cardiomyocytes
- Figure 2.2 Effect of ALN on $[Ca^{2+}]_i$ dynamics in HL-1 atrial cardiomyocytes
- Figure 2.3 Alendronate acutely modified $[Ca^{2+}]_i$ dynamics in HL-1 atrial cardiomyocytes
- Figure 2.4 Acute effect of ALN on caffeine-induced Ca^{2+} responses in HL-1 atrial cardiomyocytes
- Figure 2.5 Long-term effect of ALN on caffeine-induced $[Ca^{2+}]_i$ responses of HL-1 atrial cardiomyocytes
- Figure 2.6 Caffeine-induced $[Ca^{2+}]_i$ responses exhibited oscillatory dynamics in HL-1 atrial cardiomyocytes exposed to ALN for 48 h
- Figure 2.7 Effect of ALN on protein prenylation in H9c2 ventricular cardiomyocytes
- Figure 2.8 Long term effects of ALN on caffeine-induced Ca^{2+} responses of H9c2 ventricular cardiomyocytes

ABBREVIATIONS

ALN = alendronate

AF = atrial fibrillation

ATP = adenosine triphosphate

AV node = atrioventricular node

BP = bisphosphonate

Ca^{2+} = calcium

$[\text{Ca}^{2+}]_i$ = intracellular free calcium concentration

CICR = calcium induced calcium release

CRT = calreticulin

CSQ = calsequestrin

FPP = farnesyl pyrophosphate

FPPS = farnesyl pyrophosphate synthase

FTI-277 = Farnesyl transferase inhibitor

GAPDH = Glyceraldehyde-3-phosphate dehydrogenase (GAPDH)

GGTI-298 = geranylgeranyltransferase inhibitor

GGPP = geranylgeranyldiphosphate

HDJ-2 = DnaJ 2 chaperon protein, known prenylation substrate

IP_3 = inositol triphosphate

Ryr = ryanodin receptor

RP-1 = Rab-RP1 small GTPase, known geranyl-geranylation substrate

SA node = sinoatrial node

SER = sarcoendoplasmic reticulum

ABSTRACT

Alendronate (ALN) is effective in the treatment of osteoporosis. However, ALN has been recently associated with an increased risk of serious atrial fibrillation. We investigated the effects of ALN on cytosolic free calcium concentration ($[Ca^{2+}]_i$) in cardiomyocytes. HL-1 atrial cardiomyocytes were loaded with fura-2 and examined using microspectrofluorimetry. ALN (10^{-8} , 10^{-7} , 10^{-6} M) induced transitory high frequency oscillations of $[Ca^{2+}]_i$ with greater frequency for 10^{-8} M ALN (61 ± 10 mHz) compared to 10^{-6} ALN (42 ± 4 mHz). In cells treated with 10^{-6} M ALN responses to subsequent application of caffeine were delayed, and exhibited a decrease in the rate and amplitude of $[Ca^{2+}]_i$ increase. Long term (48 h) exposure to 10^{-8} M Alendronate resulted in delay of caffeine-induced Ca^{2+} transients and decreased rate of $[Ca^{2+}]_i$ increase, followed by oscillations in $[Ca^{2+}]_i$ of 54 ± 8 mHz versus those observed at higher concentrations of Alendronate (35 ± 5 mHz). Changes in calcium dynamics were accompanied by significant changes in the expression of sarcoendoplasmic reticulum ATPase (SERCA2a), calsequestrin and calreticulin.

RÉSUMÉ

Alendronate est efficace dans le traitement de l'ostéoporose. Alendronate a récemment été associé avec un risque élevé de fibrillation auriculaire sévère. On a examiné les effets d'Alendronate sur la concentration de calcium cytosolique ($[Ca^{2+}]_i$) dans les cellules musculaires cardiaques. Les cellules musculaires cardiaques HL-1 étaient chargées avec Fura-2 et examinées par microspectrofluorimétrie. Alendronate (10^{-8} , 10^{-7} , 10^{-6} M) ont provoqué des oscillations de $[Ca^{2+}]_i$ fugaces et haute fréquence à 10^{-8} M Alendronate (61 ± 10 mHz) comparé aux concentrations plus hautes (42 ± 4 mHz). Dans les cellules traitées avec 10^{-6} M ALN, la réponse à l'application de caféine était avec délai, et a manifesté une diminution dans la fréquence et l'amplitude d'augmentation de $[Ca^{2+}]_i$. L'exposition à l'ALN à long terme (48 h) ont provoqué un délai des élévations de calcium transitoires, et une diminution de la fréquence d'augmentation de $[Ca^{2+}]_i$ suite aux oscillations de $[Ca^{2+}]_i$, caractérisés par une augmentation de fréquence avec 10^{-8} M Alendronate (54 ± 8 mHz) comparé aux concentrations plus hautes (35 ± 5 mHz). Le changement des dynamiques de calcium étaient accompagnés par les changements considérables dans l'expression d'ATPase (SERCA2a), calsequestrin et calreticuline du réticulum sarcoendoplasmique.

ACKNOWLEDGEMENTS

This thesis would not have been possible without my supervisor, Dr. Svetlana Komarova. I would like to express my deep gratitude to Dr. Komarova for her guidance, encouragement, enthusiasm and inspiration. I am indebted to her for the opportunity to work with her.

I thank Dr. Lorraine Chalifour, Amanda Kasneci of the Division of Experimental Medicine, Faculty of Medicine, McGill University and Dr. Gustavo Duque and Daniel Rivas of the Aging Bone Research Program, Nepean Clinical School, University of Sydney for collaborating with us on this project.

I would also like to thank my fellow lab members for their help and camaraderie. Especially thank you to Jenna Fong who helped me translate my abstract. Thank you to Scott Bunnell for allowing me to store my data on his back up system and for the computer advice.

I thank Dr. P. Tupper, Department of Mathematics and Statistics, McGill University, Montreal, Canada, for assistance in FTA analysis. I thank Dr. J. Galipeau, Lady Davis Institute for Medical Research, Montreal, Canada for providing cell lines used in this study and Merck Pharmaceuticals for providing Alendronate.

Finally, I thank my family for their loving support, especially my husband, Matty Suss, for his encouragement, support and patience.

This study was supported by CIHR Strategic Training Program in Skeletal Health Research. This study was also funded by grants from the University of Sydney Medical Research Foundation (to Dr. Duque), the Nepean Medical Research Foundation (to Dr. Duque), the Canadian Institutes for Health Research (to Dr. Duque and Dr. Komarova) and the Natural Sciences and Engineering Research Council (to Dr. Chalifour and Dr. Komarova).

CONTRIBUTIONS

Figure 5G, Figure 7 and Figure 8H are the work of Amanda Kasneci

Figure 1 is the work of Daniel Rivas

CHAPTER I – LITERATURE REVIEW

INTRODUCTION

Osteoporosis is a disorder characterized by bone fragility due to a reduction in both bone quantity and quality, which predisposes to fractures and increases mortality in older adults ¹. Currently Bisphosphonates are the most effective treatment for osteoporosis due to their efficacy in fracture prevention ². Until recently, Bisphosphonates were considered relatively safe due to the low incidence of side effects, which include esophagitis, transient hypocalcaemia and severe but infrequent osteonecrosis of the jaw ³. However, recent studies have reported an unexpected increase in the incidence of serious atrial fibrillation (AF) in patients treated with Zoledronate ⁴ and later in patients treated with alendronate ⁵. At least one of the subsequent population studies also reported a strong association between the use of alendronate and an incidence of AF ⁶. In studies linking the use of Bisphosphonates with AF, two features are of note: Firstly, the use of both Zoledronate and Alendronate was associated with an increase in the number of serious AF events (classified as sustained and characterized as life threatening, resulting in hospitalization or death) ^{4,5}. Use of Alendronate was associated with an increased risk of AF events, approximately 3% of AF events in the study reported by Heckbert et al could be due Alendronate use⁷. Secondly, most cases of AF did not occur immediately after treatment, but were delayed by 30 days or more ^{4,6}. Even though the absolute risk of AF remains very small, the wide use of bisphosphonates (22 millions of

alendronate prescriptions a year in the United States alone ⁸), necessitates better understanding of potential arrhythmogenic action of these drugs in order to identify the population at risk and to develop strategies of prevention of this unexpected side effect.

1.1 Bisphosphonates

1.1.1 General Overview

Bisphosphonates (BPs) are the most common class of drugs used in the treatment of post menopausal osteoporosis. It is known that BPs are targeted to the bone surface by their attraction to elemental calcium and cleared from circulation quickly due to a high affinity with calcium. BPs are released in the highly acidic environment of the osteoclast resorption lacunae ^{9,10}. The high negative charge of BPs usually renders them membrane impermeable however BPs can still be internalized by actively resorbing osteoclasts, which can internalize negative charged compounds by endocytosis¹¹.

In addition to osteoporosis, BPs are also often used in the treatment of other diseases characterized by excessive bone resorption, such as Paget's disease of bone and skeletal metastases from breast and prostate cancers¹¹.

1.1.2 Bisphosphonate Structure

BPs all share the common structure that is characterized by a carbon atom covalently bound to 2 phosphate groups and 2 side chains, R_1 and R_2 ¹¹. There are many variations of R_1 and R_2 and this is what gives rise to differences in the mechanism of action and anti resorptive properties between individual BPs¹¹. One great difference in the side chains divides bisphosphonates into 2 classes; Simple and Nitrogen containing BPs¹¹. Nitrogen containing BP side chains contain Amino-Alkyl and/or heterocyclic groups, hence the name¹¹. The mechanism of action on preventing bone resorption of each class differs significantly¹¹.

1.1.3 Simple Bisphosphonates

Simple BPs closely resemble pyrophosphate (PPi) due to the simple structure of their side chains¹¹. PPi is an inorganic endogenous bone mineralization regulator¹¹. Due to their similarity to PPi, simple BPs are degraded intracellularly into methylene-containing analogues of ATP¹¹. These analogues are non-hydrolysable and thus accumulate in the osteoclasts. Methylene-containing analogues of ATP reduce mitochondria membrane potential and activate caspase-3 (an apoptosis inducing kinase), inducing osteoclast apoptosis. In the presence of a caspase inhibitor, simple BPs can no longer potently prevent bone resorption¹¹. Thus, simple BPs prevent bone resorption by inducing osteoclast apoptosis.

1.1.4 Nitrogen Containing Bisphosphonates

In contrast to simple BPs, Nitrogen containing BPs cannot be metabolized due to large R₂ side chains¹¹. Instead, Nitrogen containing BPs have been shown to inhibit farnesyl pyrophosphate synthase (FPPS), the enzyme important in isoprenylation (farnesylation and geranylation) of small GTPases, such as Rac, Ras, Rab, and Rho, leading to cytoskeleton disruption, inhibition of osteoclast differentiation and activity, as well as induction of apoptosis^{9,12,13}. Furthermore, bisphosphonates were shown to act as potent inhibitors of both protein geranylation and farnesylation in other cell types such as cancer cells¹⁴. Nitrogen containing BPs thus prevent bone resorption mainly by inhibiting the mevalonate pathway thereby preventing osteoclast resorption¹².

1.1.5 Side Effects

Side effects include esophagitis, transient hypocalcaemia, flu-like symptoms, severe but infrequent osteonecrosis of the jaw³. The main target of bisphosphonates are osteoclasts, which participate in plasma calcium homeostasis. It has been reported that bisphosphonates induce transient hypocalcaemia in small number of patients, which is asymptomatic and generally resolved within 30 days^{4,5}. It has been shown that bisphosphonates increase the levels of inflammatory cytokines¹⁵. The cytokine release occurs soon after bisphosphonate administration, leading to acute side effects such as fever and influenza-like symptoms¹⁵. Theoretically, recently identified association of AF with Bisphosphonates treatment can be related to other known side effects, such

as hypocalcaemia, or inflammation¹⁶. However, in all studies the risk for AF was found to increase with time, thus occurring after inflammation and hypocalcaemia are resolved⁷. Thus, the possibility of direct effects of bisphosphonates on cardiomyocytes is plausible.

1.2 Heart Physiology and Calcium

1.2.1 Structure of The Heart

The heart is a muscular organ that functions as the body's motor. The heart pumps blood containing oxygen as well as hormones and other important molecules throughout the body via the circulatory system¹⁷. A healthy heart will pump at a steady rate that can be modified to suit bodily needs (i.e. exercise). The heart rhythm is robust since an abnormal disruption of its pattern, even for a short period, can cause irreparable damage to the body and the heart itself¹⁷.

The human heart is composed of 4 chambers¹⁷. The upper two, the atria, form a weaker pump, and the lower two, the ventricles form a second, stronger pump¹⁷. Although the heart contains several different cell types including highly oxidative, involuntary muscle¹⁷. The walls of four chambers are composed of a mesh of cardiomyocytes¹⁷. The right side of the heart serves to collect deoxygenated blood from the body¹⁷. Blood collects into the right atria and is pumped into the right ventricle¹⁷. The right ventricle pumps blood into the lungs for carbon dioxide drop off and oxygen pick up¹⁷. Freshly oxygenated blood is collected into the left atria from the lungs and is pumped into the left ventricle which pumps out to the

entire body¹⁷. The left side of the heart must pump blood out with enough force to reach all the extremities¹⁷.

Underlying each heart beat is a coordinated series of events known as the cardiac cycle: the atrial diastole (atrium contracts), the ventricular diastole (ventricles contract) followed by a complete cardiac diastole (relaxation of all the heart muscle)¹⁷.

1.2.2 Electrical Activity in The Heart

The cardiac cycle is coordinated by an electrical impulse which spreads throughout the heart in an organized manner, stimulating its contraction¹⁸. Normal electrical conduction in the heart begins with an action potential generated by the sinoatrial (SA) node, a small section of specialized cardiac cells located on the right atrium wall¹⁸. The SA node is responsible for initiating each heart beat and setting the pace for heart rate, basically acting as a pacemaker¹⁸.

All cardiomyocytes have the ability to generate electrical impulses due to stochastic opening and closing of ion channels in the myocyte cell membrane (sacrolemma)¹⁸. However the cells that make up the SA node generate impulses at a rate that is slightly faster than other cardiac myocytes¹⁸. SA node cells also differ from cardiac myocytes by the fact that they do not contract¹⁸.

Cardiac myocytes have a negative membrane potential under resting conditions. The action potential generated by the SA node serves to depolarize the myocyte membrane rendering it more positive¹⁸. In the healthy heart cardiac myocytes are attached adjacently by intercalated discs allowing for cardiac muscle to behave as an electrochemical syncytium thereby connecting the potential of sarcolemma of the myocytes^{17 18}. Electrical activity can propagate easily from cell to cell and thus throughout the heart¹⁷.

Each action potential spreads from the right atria to the left atria, stimulating their contraction and then tends toward the atrioventricular (AV) node where it is delayed to allow for the atria to dispel all blood into the ventricles before the ventricles contract¹⁷. The action potential is then passed through specialized conduction fibers, towards the apex of the heart and finally to the ventricular epicardium¹⁷.

1.2.3 Calcium

Calcium is a molecule that plays a central role in the regulation of important physiological functions such as cell growth, cell proliferation, cell lifespan, hormone release and cardiac contraction¹⁹. Cell surface receptors and/or cell membrane voltage changes can initiate acute increases in intracellular calcium in the entire cell or localized intracellular areas eliciting physiological responses. This is why intracellular calcium concentration is strictly regulated. Under resting

conditions intracellular calcium concentration is approximately 100 nM, despite millimolar levels of extracellular calcium²⁰.

1.2.4 Important Regulators of Calcium Dynamics in Cardiomyocytes

At the cellular level it is calcium that relates membrane depolarization with cardiomyocyte contraction. When the action potential reaches the cardiomyocyte membrane it leads to a rise in cytosolic free calcium concentration ($[Ca^{2+}]_i$) that initiates cell contraction²¹. Upon membrane depolarization, cardiomyocytes undergo a process known as calcium induced calcium release (CICR)²¹. Depolarization triggers the voltage gated sarcolemma L-type receptor, a calcium channel, to open²¹. For cardiomyocytes to undergo the contraction, cytosolic calcium must increase by 100 μ M during the depolarization in order to release calcium from intracellular stores²⁰. Ryanodine receptors (Ryr) are generously dispersed on the sarcoendoplasmic reticulum (SER), a specialized endoplasmic reticulum in myocytes²¹. The SER has several functions including lipid synthesis, protein folding, post translational modifications and calcium storage²¹. Ryr are SER calcium channels that are sensitive to calcium²². The 100 μ M rise in $[Ca^{2+}]_i$ triggers the Ryr to open leading to a large release of calcium from the SER²². In turn calcium binds to troponinC in contractile machinery causing actin and myosin proteins to crawl along each other [walker et al]. The result of these events is contraction of myofibrils which shortens the entire cardiomyocyte²².

For calcium to return to diastolic levels (the relaxed state), it is expelled from the cell via the sarcolemma $\text{Na}^+/\text{Ca}^{2+}$ exchanger and is resequenced back to the SER by the action of the SER ATPase (SERCA2a) ²³. Calcium is stored in the SER by low-affinity high-capacity calsequestrin (CSQ) binding ²⁴. Calreticulin (CRT) is the main calcium storage protein of the endoplasmic reticulum ¹⁹.

1.2.5 Serca

SERCA is a calcium atpase that transfers calcium from the cytosol of the cell to the SER lumen by ATP hydrolysis during muscle relaxation ²¹. Serca is controlled and negatively inhibited by phospholamban, which in turn is regulated by β -adrenergic receptors ²¹.

1.2.6 Calsequestrin

Calsequestrin is the major storage protein in the SER and binds calcium in the SER lumen thereby reducing the gradient of free calcium against which SERCA must pump and preventing precipitation ²⁵. CSQ can store a very large amount of calcium ²⁶. During the systole (contraction) each molecule of CSQ can release ~4050 calcium ions ²⁶. CSQ plays a very important role in CICR as it is part of a quaternary complex with the Ryr2 (Ryr2 in cardiomyocytes), triadin and junctin. At low SER luminal $[\text{Ca}^{2+}]_i$, CSQ is present as a monomer associated with regulatory proteins, Triadin and Junctin. At high calcium concentrations, CSQ

monomers form a polymer and dissociate from Junctin and Triadin. The complex functions to control calcium release via the Ryr²⁵. Binding of Ryr with calcium triggers CSQ to free previously bound calcium so it can be passed through the Ryr receptor channel into the cytosol²⁵. Defects in this complex can lead to cardiac arrhythmias due to altered regulation of the Ryr calcium release channel²⁵.

1.2.7 Calreticulin

Calreticulin is a calcium binding ER (endoplasmic reticulum) chaperone protein whose functions include folding and assembly of newly synthesized proteins in a calcium dependent manner as well as a calcium buffer¹⁹. The C-terminal domain of CRT binds calcium with low affinity and high capacity¹⁹. The C-domain both acts as a calcium sensor that regulates its interaction with other proteins as well as storing calcium¹⁹. CRT releases calcium upon binding of inositol triphosphate (IP₃) with the ER IP₃ receptor. The IP₃ receptor is similar to the Ryr, and serves as a channel through which calcium can pass to the cytosol¹⁹.

1.2.8 Caffeine as a Stimulus

Caffeine activates the Ryr by increasing Ryr receptor sensitivity to calcium. This allows for the Ryr receptor to be activated by already present basal free calcium²⁷. Caffeine is routinely used as an indicator of SER capacity for Ca²⁺

²⁷. In addition, at lower concentrations caffeine is used to stimulate Ca^{2+} release from Ryr-dependent stores ²⁷.

1.2.9 Atrial and Ventricular Cardiomyocytes

The CICR cycle described above is the same for all cardiomyocytes. However the cardiomyocytes of the atria, atrial myocytes, differ from the those of the ventricles, ventricular myocytes. These differences are structural and result in a different calcium response pattern to depolarization ¹⁸. The most noted structural difference between the two cardiomyocyte types is that atrial cardiomyocytes do not contain transverse-tubules (T-tubules) while ventricular cardiomyocytes do ¹⁸. T-tubules are invaginations of the sarcolemma that bring L-type calcium channels in extremely close proximity to Ryr receptors in ventricular myocytes¹⁸. As a result of a lack of T-tubules in atrial myocytes, calcium release into cytosol through the sarcolemma must travel some ways inwardly to Ryr receptors on the sarcoplasmic reticulum ¹⁸. Rate of movement of the calcium inwards determines the extent of contraction and on a larger scale the force of atrial pumping ¹⁸. The offset and magnitude of the calcium released from the SER is thus a function of how quickly calcium can travel centripetally to the Ryr from the L-type receptor in the sarcolemma ¹⁸. Hormones and proteins that aid or inhibit this process thus have control over the magnitude and rate of atrial cardiomyocyte contraction ¹⁸.

1.3 Atrial Fibrillation

Atrial Fibrillation (AF) is defined as a lack of a normal atrial systole due to uncoordinated, random electrical activity in the atrium²⁸. AF will cause a rapid and irregular heartbeat and is potentially very dangerous, since irregular atrial contraction disrupts normal blood flow through the atria²⁸. Although a large percentage of blood can load into the ventricles in the absence of an atrial systole due to venous pressure, 10 - 30% of blood must be pumped via the atria into the ventricles¹⁸. Lack of coordinated atrial contraction leads to improper expelling of the atria allowing blood to stagnate, which can lead to thrombus formation¹⁸. The most morbid effect of AF is stroke due to an embolism resulting in significant mortality^{18 28}. AF may result from abnormal electrical conduction and/ or activity in the atrium²⁸. AF is classified as in three categories; transitory (7 days or less, no reoccurrence in subsequent 6 months), persistent/ intermittent (more than 7 days or if AF reoccurred within 6 months along with having periods of returned atrial systole) and sustained (continuous AF during 6 months after episode)⁷. AF is initiated and maintained in several ways. First, atrial myocytes can depolarize independently of the action potential generated by the SA node^{7,28}. Second, chaotic electrical activity in the atria can shorten the delay between subsequent depolarizations during which the membrane normally cannot be depolarized^{7,28}. This worsens AF and can bring it to a sustained level^{7,28}. Finally, sections of the atria may not be conducting the action potential initiated at the SA node⁷. In the cases of chronic arrhythmias these sections influence properly conducting areas eventually overriding the SA node 'pacemaker' and increasing

the area of abnormally conduction and allowing the AF to endure⁷. At the cellular level, it has been also shown that spontaneous calcium activity can be associated with arrhythmogenesis^{23,29,30}.

1.4 Objective and Rationale

Osteoporosis is a debilitating disease characterized by excessive bone resorption leading to compromised bone mineral density. ALN has been associated with increased risk of AF. Although it is possible that ALN can affect cardiac function indirectly, by disturbing blood mineral composition or increasing the levels of inflammatory cytokines, the timing of AF development does not coincide with other side effects associated with treatment.

The objective of this study was to assess if the direct effects of ALN on cardiac cells are biologically plausible. We have used an *in vitro* model to assess the effect of ALN on protein isoprenylation, expression of calcium homeostasis proteins and calcium dynamics in cardiomyocytes from both atrial and ventricular origin.

CHAPTER II – MATERIALS AND METHODS

2.1 Reagents

ALN was provided by Merck Pharmaceuticals (Whitehouse Station, NJ, USA). ALN was dissolved in phosphate-buffered saline (PBS), the pH was adjusted to 7.4 with 1N NaOH and then solution was sterilized through a 0.2 μm filter. Farnesyl transferase inhibitor (FTI-277) and geranylgeranyltransferase inhibitor (GGTI-298) were purchased from Sigma-Aldrich (St. Louis, Missouri, USA). Immobilon P membrane was purchased from Millipore (Bedford, MA). Calsequestrin (CSQ), Calreticulin (CRT) and sarcoendoplasmic reticulum ATPase 2a (SERCA2a) polyclonal antibodies were from Affinity BioReagents (Golden, CO). Glyceraldehyde-3-phosphate dehydrogenase (GAPDH) antibody was from Sigma-Aldrich. DnaJ 2 (HDJ-2) antibodies were from Lab Vision (Fremont, CA, USA) and Rab-RP1 (RP-1) antibodies were from Santa Cruz Biotechnology (Santa Cruz, CA, USA). Secondary antibodies and enhanced chemiluminescent detection kits were from Pierce (Rockford, IL). Fura-2 was from InVitrogen, (Carlsbad, CA). Other reagents were from Sigma-Aldrich (St. Louis, MI) unless otherwise noted.

2.2 Cell culture

Mouse atrial cardiomyocyte HL-1 cells³¹, were kindly provided by Dr. Jacques Galipeau (Lady Davis Institute for Medical Research, Montreal, Canada). Cells

were plated on dishes coated with 25 g/ml fibronectin/0.02% gelatin and maintained at 37°C in a humidified atmosphere with 5% CO₂ in Claycomb Media (SAFC BioSciences, Arkansas) supplemented with 10% fetal bovine serum (BioWhittaker), 4 mM L-glutamine, 100 µM norepinephrine (Sigma-Aldrich), 100 units/ml penicillin, 100 µg/ml streptomycin (Life Technologies), which was changed every 2 days.

Rat ventricular cardiomyocyte H9c2 cells³² were purchased from the American Type Culture Collection, (ATCC CRL1446, Rockville, MD, USA) and grown at 37°C in a humidified atmosphere with 5% CO₂ in Dulbecco's modified Eagle's medium supplemented with 10% fetal bovine serum, 2 mM L-glutamine, 1% nonessential amino acids, 100 units/ml penicillin, and 100 µg/ml streptomycin as previously described³³. To induce cardiac differentiation, H9c2 cells were treated for 2 days with reduced serum (1%) and daily additions of retinoic acid (10⁻⁸ M).

2.3 Alendronate Treatments

HL-1 cells were grown to 90% confluency. Then either calcium dynamics were measured, or media was changed and supplemented with vehicle (PBS), increasing concentrations of ALN (10⁻⁸, 10⁻⁷, 10⁻⁶ M), FTI-277 (5-10 µM) or GGTI-298 (5-10 µM). After 48 hours of treatment, cells were used either for analysis of protein expression and prenylation, or to measure calcium dynamics.

Cardiac differentiated H9c2 cells were supplemented with vehicle (PBS),

increasing concentrations of ALN (10^{-8} , 10^{-7} , 10^{-6} M), FTI-277 (5-10 μ M) or GGTI-298 (5 μ M). After 48 hours of treatment, cells were used either for analysis of protein expression and prenylation, or to measure calcium dynamics.

2.4 Protein isolation and immunoblot analysis

For DnaJ 2 (HDJ-2), and Rab-RP1 (RP-1), cells were lysed in 20 mM tris-HCl, pH 7.5, 200 mM DTT, 200 mM KCl, 0.5 ml glycerol and protease inhibitor tablets (Roche Diagnostics Canada, Laval, QC, Canada), freeze-thawed 3 times in a dry ice-ethanol bath and centrifuged at 11500 rpm for 15 minutes to remove insoluble material. Cell lysates were dissolved in SDS electrophoresis buffer (Bio-Rad, Hercules, CA, USA) and proteins separated on SDS-polyacrylamide gels and subsequently electrotransferred to polyvinylidene difluoride membranes. Membranes were blocked with PBS containing 0.1% Tween 20 and 10% non-fat dry milk, incubated overnight at 4°C using an antibody directed against either human DnaJ 2 (HDJ-2), unprenylated Rab-RP1 (RAP-1), GAPDH or τ -tubulin. The bound antibodies were detected with the corresponding secondary antibodies conjugated with horse radish peroxidase.

For calcium homeostasis proteins, cells were homogenized in 500 μ l of 1xSDS lysis buffer (62.5 mM Tris pH 6.8, 2% w/v SDS, 10% glycerol, 50 mM DTT, 0.01% w/v bromophenol blue). Homogenates were incubated on ice for 2 h, centrifuged at 10,000 X g for 5 min at 4°C and used in immunoblots without further manipulation. Protein concentrations were determined using the Bio-Rad

Protein Determination Assay (BioRad, Hercules, CA), and protein was electrophoresed through SDS-PAGE and electrophorically transferred to Immobilon P membranes. Membranes were stained with Ponceau S to confirm equivalent protein loading and transfer. Membranes were blocked for 2 hours in TBST+milk ((20 mM Tris pH 7.5, 150 mM NaCl, 0.02% Tween 20) + 3% skim milk powder). CSQ antibody was diluted 1:2500, SERCA2a and CRT 1:500 and GAPDH 1:10000 in TBST+3% milk and incubated overnight at 4°C. Membranes were washed in TBST, incubated for 2 h at room temperature with horseradish-peroxidase-coupled secondary antibodies diluted 1:20000 in TBST+milk, washed, and visualized with chemiluminescence substrates according to the manufacturer's instructions.

Blots were developed by enhanced chemiluminescence using Perkin-Elmer reagents (Perkin-Elmer, Boston, MA, USA). X-ray films were scanned using an HP Scanjet 5100 C and HP Precision Scan Software (Hewlett-Packard, Palo Alto CA), and the areas under the peaks were quantified using ScionImage Release Beta 3 Software (National Institutes of Health, Bethesda, MD). Test protein expression was standardized to the signal from GAPDH or τ -tubulin measured on the same blot.

2.5 Fluorescence Measurement of Cytosolic Free Ca^{2+} Concentration

$[\text{Ca}^{2+}]_i$ of H9c2 and HL-1 cells was monitored using microspectrofluorimetry³⁴. Cells grown on 35 mm glass bottom dishes (MatTek) were loaded with 1.5 mM

fura-2-AM (Invitrogen) for 40 min at room temperature in loading medium (DMEM supplemented with 10 mM HEPES). At the end of the loading period, the media was replaced with physiological buffer, normal Tyrodes solution, containing 130 mM NaCl; 5 mM KCl; 10 mM glucose; 1 mM MgCl₂; 1 mM CaCl₂; 20 mM HEPES; adjusted to pH 7.4 with NaOH, and the dishes were mounted onto the stage of an inverted phase-contrast microscope (Nikon, T-2000). The measurements were performed at room temperature. Changes in fluorescent emission at 510 nm, following alternate excitation at 340 and 380 nm (managed by high-speed wavelength-switching device, Lambda DG-4; Quorum Technologies) were recorded using a cooled CCD camera (Hamamatsu), collected and analyzed using image analysis software (VLOCITY, Improvion). Caffeine (0.5 mM) and ALN (10⁻⁸, 10⁻⁷, 10⁻⁶ M) were administered by bath application.

2.6 Spectral analysis of calcium oscillations

We analyzed periodicity of calcium oscillations using Fourier Transform Analysis (FTA) ³⁵. Calcium traces were truncated to concentrate on the region exhibiting oscillatory behavior, which resulted in the time series 50 - 140 s long. The trend (smooth component of the transient) was identified using a least square approximation and subtracted from these segments. The FTA of resulting time series were computed using the Fast Fourier Transform in Matlab (Mathworks Inc.). Spectral densities for each frequency f_i was computed as $|f_i|^2 / \sum_i |f_i|^2$. Frequencies lower than 20 mHz were considered irrelevant, since the

corresponding period was comparable to the length of the segments analyzed.

It should be noted that to ensure that the data was not aliased, a sampling rate of 3 Hz was used to ensure it was above the Nyquist frequency of the highest possible HI-1 beating frequency.

2.7 Statistical analysis

Data are presented as representative traces, representative immunoblots, or as mean \pm SEM with sample size n indicating the number of independent experiments, or the number of cells analysed for calcium studies. Statistical comparisons were based on a Student's t-test or a χ^2 test, and accepted as statistically significant at $p < 0.05$.

CHAPTER III RESULTS

3.1 Effect of Alendronate on Farnesylation/Geranylation in HL-1 Atrial Cardiomyocytes

Previously, the mouse HL-1 cell line has shown to retain phenotypical characteristics of atrial cardiomyocytes³¹. We used HL-1 cells to assess whether ALN directly affects protein prenylation in HL-1 cells. We examined the effect of ALN on the expression of accepted markers of farnesylation, HDJ-2 and geranylation, RAP-1³⁶ and compared it to the effects of pharmacological inhibitors of farnesyl transferase, FTI-277, and geranyl geranyl transferase, GGTI-298 (Fig. 1). We have found that ALN did not affect HDJ-2 farnesylation, whereas inhibition of farnesyl transferase by FTI-277 did affect HDJ-2 farnesylation and resulted in unfarnezylated HDJ-2 (Fig. 1A). In contrast, ALN inhibited geranylation of RAP-1 in HL-1 cells. ALN increased the amount of unprenylated RAP-1 (Fig. 1B). The effect of ALN was similar to the effect of specific geranyl geranyl transferase inhibitor GGTI-298. Both ALN and GGTI-298 had an additive effect on RAP-1 geranylation (Fig. 1B).

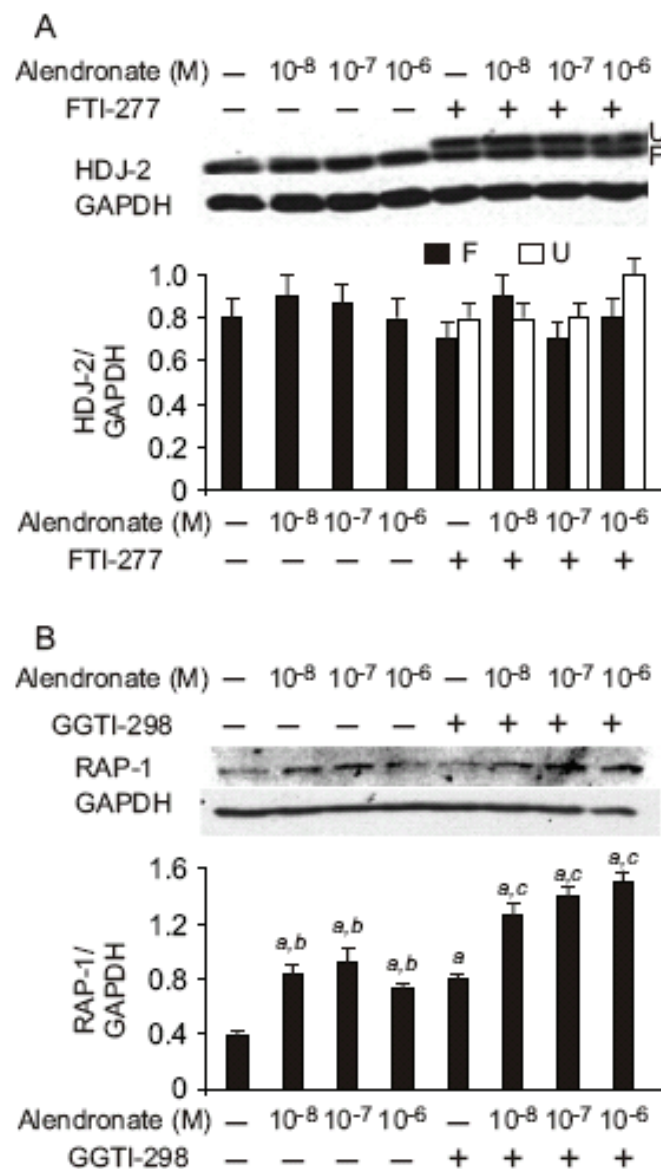


Figure 1. Effect of ALN on protein farnesylation and geranylation in HL-1 atrial cardiomyocytes

HL-1 cells were treated for 48 h with vehicle (-), ALN (10⁻⁸, 10⁻⁷ or 10⁻⁶ M), FTI-277 (5 μ M), GGTI-298 (5 μ M) or a combination of ALN with FTI-277 or GGTI-298, then cell lysates were collected and immunoblotted for HDJ-2 (A) or unprenylated Rab-RP1(RAP-1) (B). GAPDH was used as a loading control. **A**, Treatment with ALN did not affect HDJ-2 farnesylation. In contrast, treatment with FTI-277 inhibited protein farnesylation independently of addition of ALN. Shown

are representative immunoblots and average levels of expression of farnesylated (F, black bars) and unfarnesylated (U, white bars) HDJ-2 normalized to GAPDH expression. **B**, ALN inhibited geranylation of RAP-1 to an extent similar to the effect of GGTI-298. The effects of ALN and GGTI-298 on RAP-1 geranylation were additive. Shown are representative immunoblots and average levels of expression of RAP-1 normalized to GAPDH expression. For A and B, data are means \pm SEM, $n = 3$ independent experiments, different letters indicate significantly different data.

3.2 Effect of Alendronate on Calcium Dynamics in Atrial Cardiomyocytes

To study the acute effects of ALN on calcium dynamics in cardiomyocytes, cells were loaded with calcium-sensitive, cell permeable dye fura-2-AM, and changes in $[Ca^{2+}]_i$ in live cells were monitored using microspectrofluorometry. HL-1 cells were imaged untreated for the first 30 s, then vehicle or ALN at concentrations 10^{-8} M, 10^{-7} M and 10^{-6} M was added via bath application (Fig. 2). Each trace on Fig. 2B-E represents changes in the average $[Ca^{2+}]_i$ of an individual cell over time. In the control condition, basal calcium was stable within first 100 seconds of imaging (Fig. 2B), and bath application of vehicle (NT) did not affect $[Ca^{2+}]_i$ (data not shown). Addition of ALN in all concentrations resulted in appearance of periodic oscillations in a subset of HL-1 cells (Fig. 2A arrow, and Fig. 2C-E). When HL-1 cells were imaged for longer than 100 s, even in untreated cultures certain percentage of cells started to exhibit random elevations of calcium. We analyzed calcium traces from both control and ALN-treated samples using Fourier Transform Analysis (FTA)³⁵. We found that significantly larger proportion of ALN-treated cells exhibited oscillatory behavior compared to untreated cells

(Fig. 3A). Interestingly, the frequency of oscillations was significantly higher in cells treated with low concentration of ALN (10^{-8} M), compared to higher concentrations (Fig. 3B). The oscillations induced by ALN calmed within 5 min after stimulation, however, the level at which $[Ca^{2+}]_i$ stabilized, was significantly lower in samples treated with ALN at 10^{-7} M and 10^{-6} M compared to untreated cells (Fig. 3C). After 48 hours of treatment with ALN, $[Ca^{2+}]_i$ recovered to levels similar to that of untreated cells (Fig. 3D). Thus, application of ALN induced transitory oscillations of $[Ca^{2+}]_i$ in atrial cardiomyocytes.

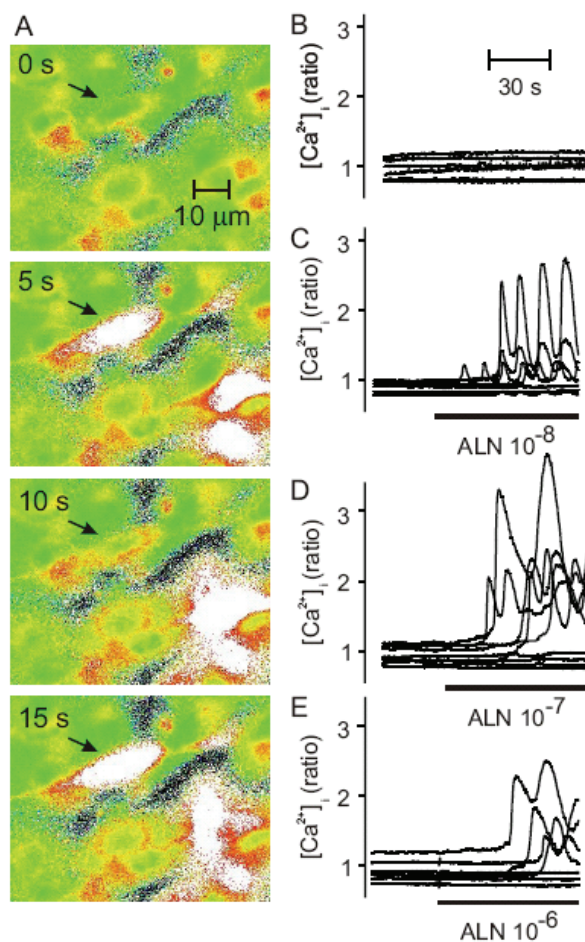


Figure 2. Effect of ALN on $[Ca^{2+}]_i$ dynamics in HL-1 atrial cardiomyocytes

HL-1 cells were loaded with fura-2 and $[Ca^{2+}]_i$ dynamics in live cells were monitored within 100 s of treatment with ALN, which was added via bath application. **A**, Micrographs demonstrate changes in $[Ca^{2+}]_i$ with time following bath addition of 10^{-8} ALN at 0 s. Levels of $[Ca^{2+}]_i$ are reflected by pseudocolor with blue/green representing low levels of $[Ca^{2+}]_i$ and red/white – high levels of $[Ca^{2+}]_i$. Arrow indicates a cell responding to ALN with oscillatory change in $[Ca^{2+}]_i$. Calibration bar applies to all images. **B**, Representative traces depict stable basal $[Ca^{2+}]_i$ levels in untreated cells. **C-E**, Administration of ALN (where indicated by the black bars) in concentrations 10^{-8} M (C), 10^{-7} M (D) and 10^{-6} M (E) induces oscillatory changes in $[Ca^{2+}]_i$ in a subset of HL-1 cells. Shown are traces from one of three independent experiments.

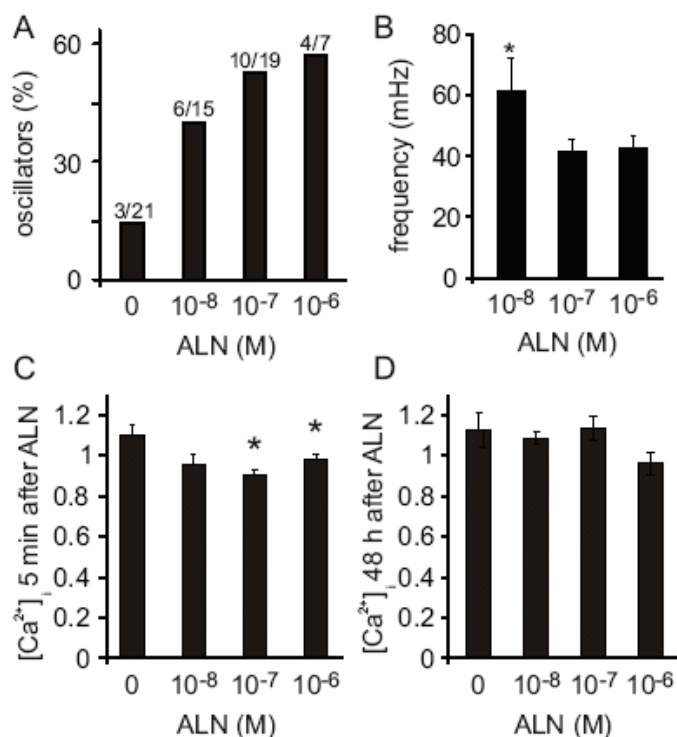


Figure 3. Alendronate acutely modified $[Ca^{2+}]_i$ dynamics in HL-1 atrial cardiomyocytes

$[Ca^{2+}]_i$ dynamic was monitored in HL-1 cells loaded with fura-2. A-B, Traces of

cells exhibiting rise in $[Ca^{2+}]_i$ within 200 s of monitoring were analyzed using FTA. **A**, Application of ALN significantly increased the proportion of cells demonstrating periodic oscillations in $[Ca^{2+}]_i$ as assessed using χ^2 test. The number of cells exhibiting significant periodicity and the total number of cells analyzed are indicated on top of the bars. **B**, Cells treated with low concentration of ALN (10^{-8} M) exhibited significantly higher frequency of oscillations compared to cells treated with higher concentrations of ALN (10^{-7} and 10^{-6} M). Data are means \pm SEM, $n = 4-10$ cells from 3 independent experiments, *indicates significant difference. **C-D**, Average levels of $[Ca^{2+}]_i$ were measured 5 minutes (C) and 48 hours (D) after treatment with ALN at indicated concentration. **C**, In most cells, 5 min after ALN application $[Ca^{2+}]_i$ stabilized, but at levels, which were significantly lower in samples treated with ALN at 10^{-7} M and 10^{-6} M compared to untreated cells. Data are means \pm SEM, $n = 15-23$ cells from 3 independent experiments, *indicates significant difference compared to untreated cells. **D**, After 48 hours of treatment, basal $[Ca^{2+}]_i$ is similar in all conditions. Data are means \pm SEM, $n = 14-21$ cells from 3 independent experiments.

3.3 Short-Term Effect of Alendronate on Caffeine-Induced Calcium

Dynamics in Atrial Cardiomyocytes

In the heart cardiac cells undergo continuous cycles of excitation and relaxation. We determined whether ALN affects calcium dynamics in HL-1 cells treated with caffeine – a ryanodine-receptor agonist that mimics calcium-induced calcium release associated with contraction³⁷. We treated cells with ALN (10^{-8} M, 10^{-7} M, and 10^{-6} M) approximately 5 minutes prior to bath administration of caffeine and then examined the changes in $[Ca^{2+}]_i$ following application of caffeine (0.5 mM) in the presence of the ALN (Fig. 4).

Untreated HL-1 cells responded to caffeine with elevations of $[Ca^{2+}]_i$ which typically peaked and then declined even in the continuous presence of caffeine (Fig. 4A). The general form of the caffeine-induced calcium transients was similar in ALN-treated cells (Fig. 4B-C). However, several parameters characterizing $[Ca^{2+}]_i$ elevation in response to caffeine (Fig. 4E) were significantly affected by acute exposure to the highest concentration of ALN (10^{-6} M): In cells exposed for 5 min to 10^{-6} M ALN the offset of calcium transients was significantly delayed. The rate of calcium increase, quantified as linear approximation of initial increase in $[Ca^{2+}]_i$, was significantly reduced. Finally, the amplitude of calcium responses, quantified as a difference between baseline and the maximum value of $[Ca^{2+}]_i$, was significantly decreased compared to untreated cells (Fig. 4F-H).

The proportion of cells responding to caffeine with a transient elevation of $[Ca^{2+}]_i$ was $24 \pm 9\%$ in control cultures, $16 \pm 3\%$ in cultures treated with 10^{-8} M ALN, $18 \pm 2\%$ in cultures treated with 10^{-7} M ALN, and significantly reduced compared to untreated cultures to $7 \pm 3\%$ in cultures treated with 10^{-6} M ALN. Thus, acute exposure to the highest concentration of ALN (10^{-6} M) significantly affected caffeine-induced calcium responses in atrial cardiomyocytes.

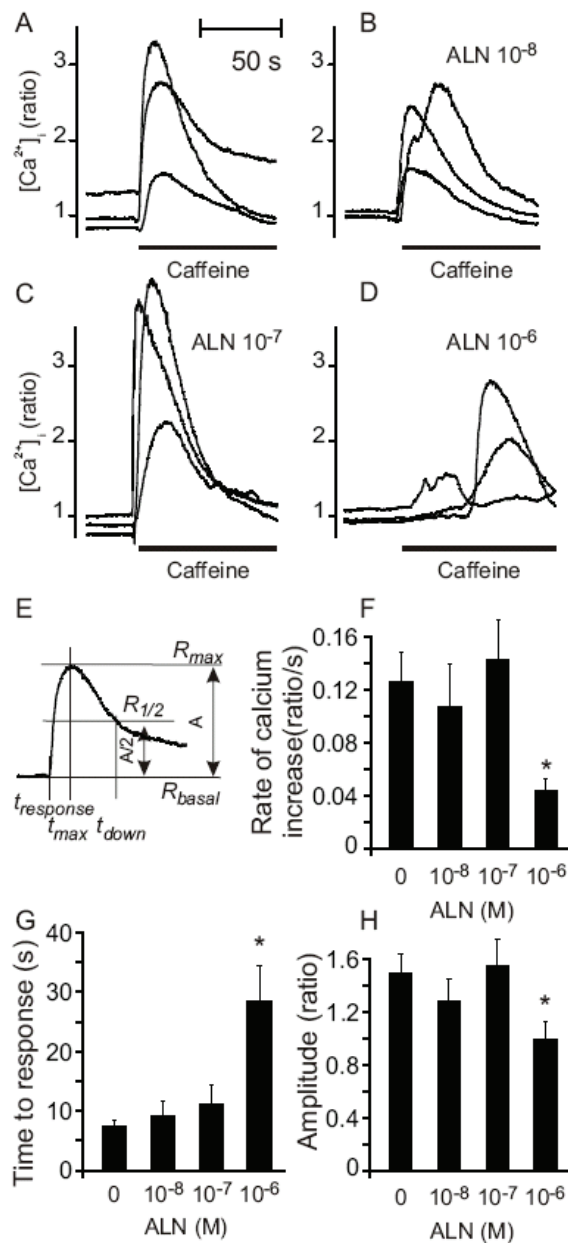


Figure 4. Acute effect of ALN on caffeine-induced Ca^{2+} responses in HL-1 atrial cardiomyocytes

HL-1 cells were loaded with fura-2, treated with ALN and ~ 5 minutes later were stimulated with caffeine (0.5 mM). **A-D**, Representative traces of caffeine-induced transient elevations of $[\text{Ca}^{2+}]_i$ in untreated HL-1 cells (A) and HL-1 cells treated with ALN at concentrations 10^{-8} M (B), 10^{-7} M (C) and 10^{-6} M (D). Administration of caffeine is indicated by the black bars. Shown are traces from

one of three independent experiments. **E**, Parameters characterizing caffeine induced Ca^{2+} transients were measured as indicated. **F**, Rate of calcium increase, quantified as $A/(t_{max}-t_{response})$, was significantly lower in HL-1 cells treated with 10^{-6} M ALN compared to untreated cells. **G**, The time to response, quantified as the time difference between the administration of caffeine and the start of the $[\text{Ca}^{2+}]_i$ transient ($t_{response}$), was significantly increased in HL-1 cells treated with 10^{-6} M ALN compared to untreated cells. **H**, Amplitude of calcium responses, A , was significantly decreased in HL-1 cells treated with 10^{-6} M ALN compared to untreated cells. For F-G, data are means \pm SEM, $n = 15-23$ cells from 3 independent experiments, * indicates significant difference compared to untreated cells.

3.4 Long-Term Effect of Alendronate on Caffeine-Induced Calcium

Dynamics in Atrial Cardiomyocytes

Since most incidence of AF in patients taking ALN occur some time after the treatment⁴, we next investigated how a longer exposure to ALN affects caffeine-induced Ca^{2+} responses. HL-1 cells were pretreated with vehicle or ALN at concentrations of 10^{-8} , 10^{-7} , and 10^{-6} M of ALN for 48 hours. Prior to loading cells with fura-2-AM for imaging ALN containing medium was washed from the cells. Changes in $[\text{Ca}^{2+}]_i$ were monitored following bath application of caffeine (0.5 mM). Stimulation of ALN-treated HL-1 cells with caffeine resulted in elevation of $[\text{Ca}^{2+}]_i$. However, the shape of the Calcium responses to caffeine of ALN-treated HL-1 cells (Fig. 5A-C) was noticeably different from that in untreated cells (Fig. 4A). Several parameters characterizing $[\text{Ca}^{2+}]_i$ elevation in response to caffeine were affected in cells treated with low concentrations of ALN: In cells treated for 48 h with 10^{-8} M ALN and to a lesser extent, with 10^{-7} M ALN, the offset of

calcium transients was delayed and the rate of calcium increase was significantly reduced (Fig. 5D, E). The amplitude of calcium responses was similar in all treatment groups (Fig. 5F).

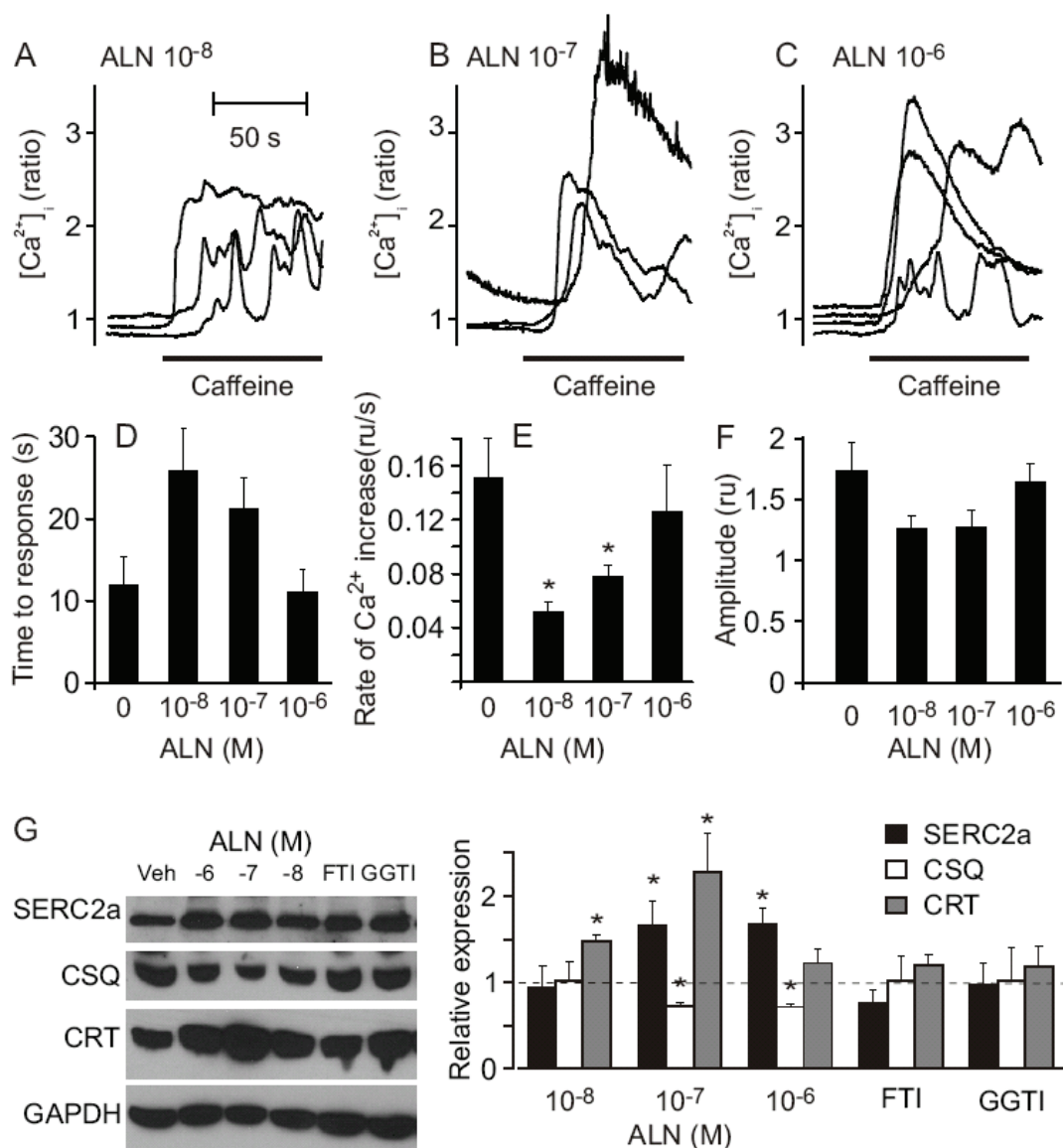


Figure 5. Long-term effect of ALN on caffeine-induced $[Ca^{2+}]_i$ responses of HL-1 atrial cardiomyocytes

HL-1 cells were treated for 48 hours with vehicle or ALN, then either $[Ca^{2+}]_i$ dynamics induced by caffeine (0.5 mM) was analyzed in fura-2-loaded cells, or whole cell protein extracts were obtained and the expression of SERCA2a, CSQ,

CRT was measured by immunoblotting. **A-C**, Representative traces of caffeine-induced $[Ca^{2+}]_i$ responses in HL-1 cells treated for 48 h with ALN in concentrations 10^{-8} M (A), 10^{-7} M (B) and 10^{-6} M (C). Administration of caffeine is indicated by the black bars. **D**, The time to caffeine-induced $[Ca^{2+}]_i$ response was increased in HL-1 cells treated for 48 h with ALN at concentrations 10^{-8} M compared to vehicle-treated cells, $p = 0.057$. **E**, The rate of calcium increase was significantly lower in HL-1 cells treated with 10^{-8} M ALN and 10^{-7} M ALN, but not in cells treated with 10^{-6} M ALN. **F**, The amplitude of caffeine-induced calcium responses was similar in vehicle treated cells and cells treated with ALN for 48 h. For D-F, data are means \pm SEM, $n = 14-21$ cells from 3-4 independent experiments, *indicates significant difference compared to vehicle-treated cells. **G**, Long-term treatment of HL-1 cells with ALN differentially affects the expression of SERCA2a, CSQ, and CRT. *Left* - Representative immunoblots from HL-1 cells treated for 48 h with vehicle (Veh), ALN (10^{-6} , 10^{-7} or 10^{-8} M), FTI-277 (10 μ M) or GGTI-298 (5 μ M), as indicated. *Right* - The expression of SERCA2a, CSQ, and CRT were normalized to the expression of GAPDH and presented relative to the levels observed in vehicle treated cells (indicated by the dashed line). Data are means \pm SEM, $n = 3$ independent experiments, *indicates significant difference compared to vehicle-treated cells.

To test whether long-term treatment with ALN has an effect on proteins involved in calcium homeostasis the expression of SERCA2a, CSQ, and CRT were measured in HL-1 cells treated for 48 h with ALN (10^{-8} , 10^{-7} , and 10^{-6} M), as well as FTI-227 and GGTI-298 (Fig. 5G). SERCA2a expression was significantly increased by treatment of HL-1 cells with ALN at doses of 10^{-6} M and 10^{-7} M, but not 10^{-8} M. CSQ expression was significantly reduced by treatment with 10^{-6} and 10^{-7} , but not 10^{-8} M ALN. In contrast, CRT expression was significantly increased by exposure of HL-1 cells to 10^{-8} M and 10^{-7} M, but not 10^{-6} M ALN. FTI-277 or

GGTI-298 had no effect on SERCA2a, CSQ or CRT expression in HL-1 cells.

The shape of caffeine-induced Ca^{2+} responses in ALN-treated cells appeared to differ from that in untreated cells (Fig. 5A-C) indicating appearance of periodic oscillations. Calcium traces were further analyzed from both control and ALN-treated samples using FTA. Calcium traces were truncated between the time of caffeine-induced maximum of $[\text{Ca}^{2+}]_i$ to the end of recordings. Next, we identified and subtracted from these segments the smooth downward component of the transient (trend) using a least square approximation. In untreated cells, a resulting transient most often contained a single wave of Ca^{2+} , arising from the deviation of an actual Ca^{2+} curve from its linear approximation (Fig. 6A *left*). In contrast, caffeine-induced $[\text{Ca}^{2+}]_i$ responses obtained in ALN-treated cells demonstrated the presence of periodic oscillations (Fig. 6B-D *left*). The FTA spectral analysis revealed a single low frequency peak in untreated cells, which corresponds to a period comparable to the length of a segment, and is therefore irrelevant (Fig. 6A *right*). In contrast, in ALN-treated cells, peaks corresponding to high frequency oscillations were evident (Fig. 6B-D, *right*). When we compared the frequencies of oscillations, we have found that at low concentration of ALN (10^{-8} M), the frequency of oscillations was significantly higher compared to higher ALN concentrations (Fig. 6E). Importantly, the frequencies of oscillations appearing in caffeine-induced responses in HL-1 cells chronically treated with ALN were similar to the frequencies of oscillations acutely induced by ALN treatment (Fig. 3B). We found that significantly larger proportion of ALN-treated

cells exhibited oscillatory component in caffeine-induced transient compared to untreated cells (Fig. 6F). Thus, we have found that atrial cardiomyocytes exposed to ALN for 48 h develop oscillations in $[Ca^{2+}]_i$ in response to caffeine treatment.

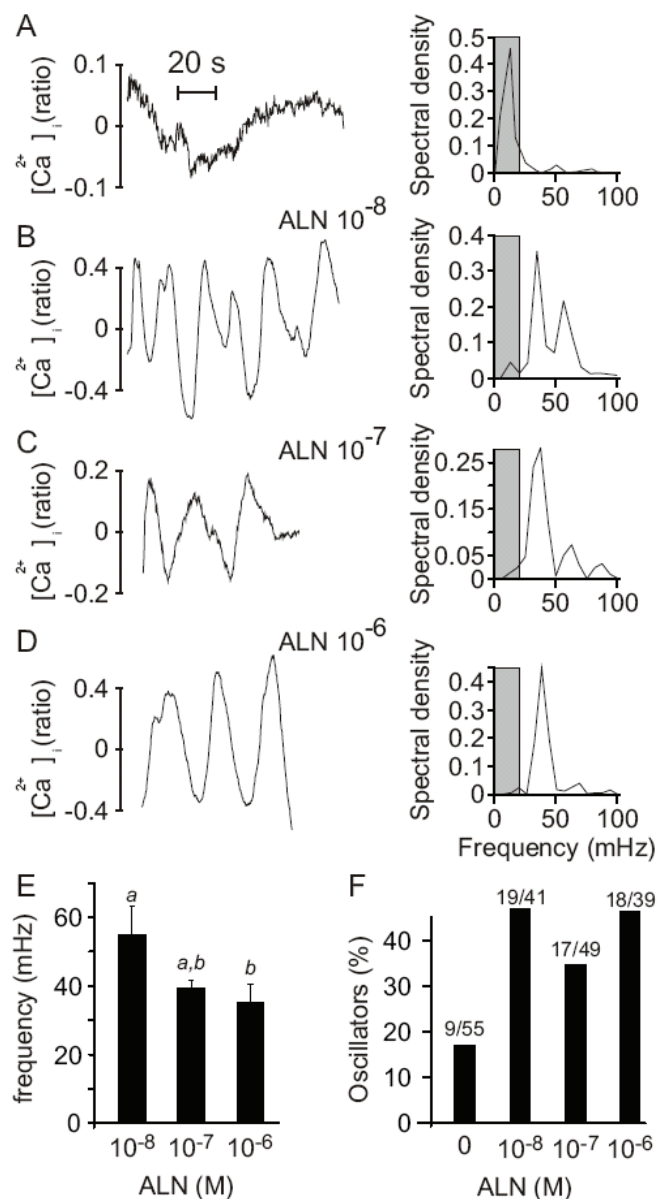


Figure 6. Caffeine-induced $[Ca^{2+}]_i$ responses exhibited oscillatory dynamics in HL-1 atrial cardiomyocytes exposed to ALN for 48 h

HL -1 cells treated with alendronate at the indicated concentrations for 48 hours, were loaded with fura-2, and stimulated with caffeine (0.5 mM). Calcium traces were truncated from the time of caffeine-induced maximum of $[Ca^{2+}]_i$ to the end of recording (60 - 140 s). The trend was identified and subtracted from these segments, which were then analyzed using FTA. **A-D, Left**, Representative traces of the detrended segments of calcium recordings in untreated HL-1 cells (A) and cells treated for 48 h with ALN at concentrations 10^{-8} M (B), 10^{-7} M (C) and 10^{-6} M (D). **Right**, Corresponding periodograms obtained using FTA, indicate dominant frequencies as narrow peaks. Spectral density corresponds to a weight of the signal with certain frequency in the whole spectrum. Grey areas indicate low frequencies that are comparable to the length of the analyzed segments and therefore irrelevant. **E**, Cells treated with low concentration of ALN (10^{-8} M) exhibited higher frequency of oscillation compared to cells treated with higher ALN concentrations (10^{-7} and 10^{-6} M). Data are means \pm SEM, $n = 3-8$ cells, different letters indicate statistically significant difference. **F**, In HL-1 cells treated with ALN for 48 h, significantly larger proportion of caffeine-induced responses was characterized by the presence of periodic oscillations, as assessed by χ^2 test. Data are percentages of cells exhibiting calcium oscillations from the total number of cells, $n = 3$ independent experiments.

3.5 Long-Term Effect of Alendronate on Ventricular Cardiomyocytes

We next examined the effects of long-term treatment with ALN on rat cardiac differentiated ventricular cardiomyocytes H9c2 cells³². We first assessed the effect of ALN on farnesylation and geranylation of markers of farnesylation, HDJ-2 and geranylation, RAP-1, and compared it to the effects of FTI-277 and GGTI-298 (Fig. 7). We have found that treatment with ALN for 48 h did not affect HDJ-2 farnesylation, whereas inhibition of farnesyl transferase by FTI-277 resulted in appearance of unfarnesylated HDJ-2 (Fig. 7A). Similarly, ALN did not affect

geranylation of RAP-1, which in these cells was also unaffected by GGTI-298 (Fig. 7B).

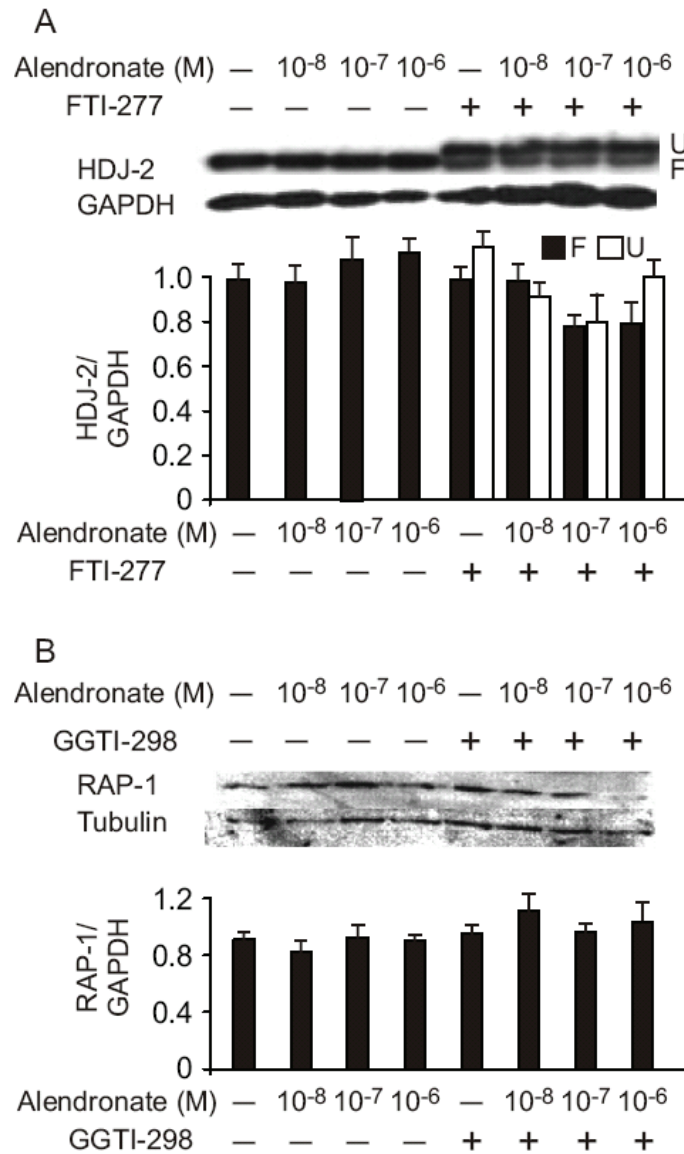


Figure 7. Effect of ALN on protein prenylation in H9c2 ventricular cardiomyocytes

H9c2 cells were treated for 48 h with vehicle (-), ALN (10⁻⁸, 10⁻⁷ or 10⁻⁶ M), FTI-227 (5 μM), GGTI-298 (5 μM) or a combination of ALN with FTI-277 or GGTI-298. Cell lysates were obtained, and HDJ-2, RAP-1 and GAPDH were detected

by immunoblotting. **A**, in H9c2 cells, ALN did not affect the farnesylation of HDJ-2, whereas FTI-277 effectively inhibited farnesylation of this protein. Shown are representative immunoblots and average levels of expression of farnesylated (F) and unfarnesylated (U) HDJ-2 normalized to GAPDH. **B**, in H9c2 cells, ALN or GGTI-298 alone or in combination did not affect geranylation of RAP-1. Shown are representative immunoblots and average levels of expression of RAP-1 normalized to GAPDH. Data are means \pm SEM, n = 3 independent experiments.

We next examined the effect of 48 h treatment of cardiac differentiated H9c2 cells with vehicle or ALN at different concentrations (10^{-8} , 10^{-7} , and 10^{-6} M) on caffeine-induced Ca^{2+} responses. Basal $[\text{Ca}^{2+}]_i$ was similar in vehicle- and ALN-treated cells. Stimulation of vehicle-treated H9c2 cells with caffeine (0.5 mM) resulted in transient elevation of $[\text{Ca}^{2+}]_i$ (Fig. 8A). Treatment with ALN for 48 h did not affect general appearance of caffeine-induced transients (Fig. 8B-D), however, the percentage of cells responding to caffeine with Ca^{2+} elevation was significantly reduced in cells treated with 10^{-8} M and 10^{-6} M ALN, compared to vehicle- or 10^{-7} M ALN-treated cells (Fig. 8E). The amplitude of the caffeine induced transients was significantly decreased in H9c2 cells treated with 10^{-8} M ALN, compared to untreated cells (Fig. 8F). The spread of the transient, quantified as the time between the offset of the transient and the time when the $[\text{Ca}^{2+}]_i$ drops to a half-maximum level, was significantly reduced in H9c2 cells treated with 10^{-7} M ALN (Fig. 8G).

We next assessed the expression of SERCA2a, CSQ, and CRT following treatment of H9c2 cells for 48 h with ALN (10^{-8} , 10^{-7} , and 10^{-6} M), as well as FTI-

227 and GGTI-298 (Fig. 8H). SERCA2a expression was significantly increased in cultures treated with 10^{-8} M ALN, but was at control levels in cells treated with 10^{-6} M and 10^{-7} M ALN. CSQ and CRT expression was increased with all concentrations of ALN. Treatment with FTI-277 resulted in a significant decrease in SERCA2a expression and a significant increase in CSQ expression, whereas GGTI-298 significantly decreased both SERCA2a and CSQ expression. CRT expression was not affected by treatment with FTI-277 or GGTI-298.

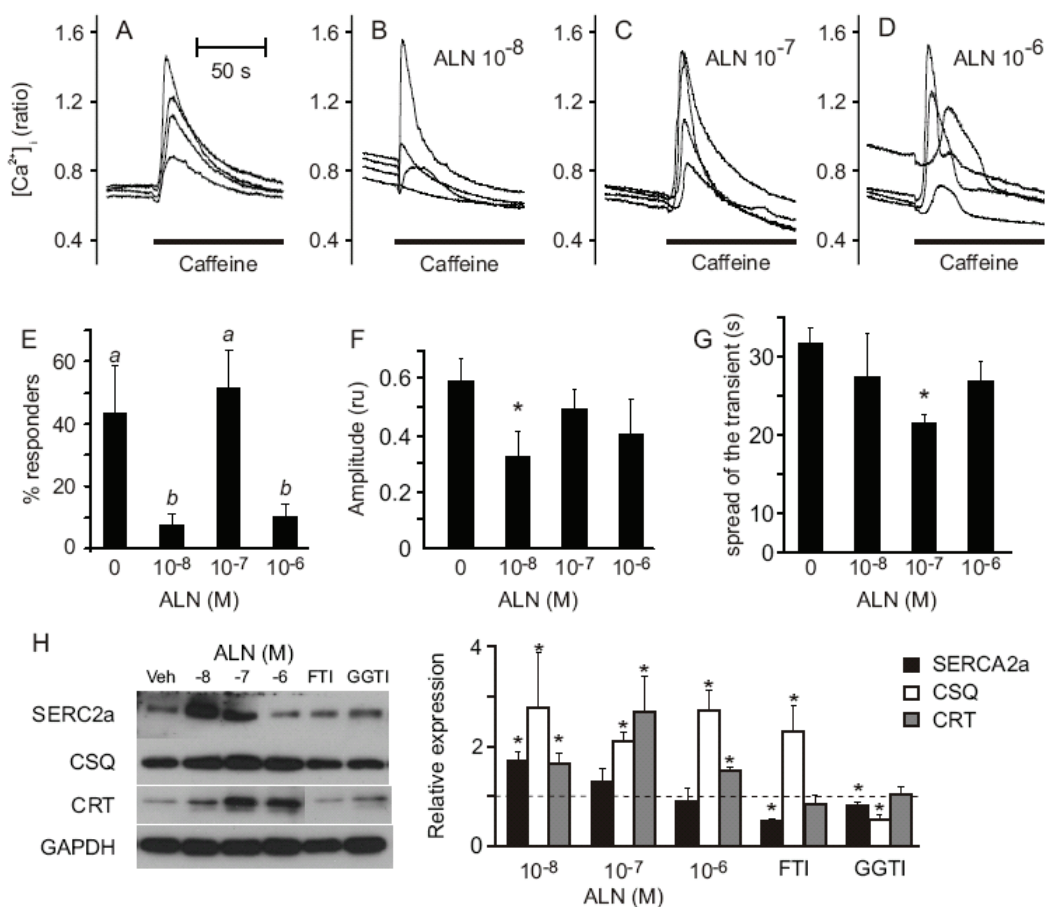


Figure 8. Long term effects of ALN on caffeine-induced Ca^{2+} responses of H9c2 ventricular cardiomyocytes

Cardiac-differentiated H9c2 cells were treated for 48 hours with vehicle or ALN, then either $[Ca^{2+}]_i$ dynamics induced by caffeine (0.5 mM) was analyzed in fura-

2-loaded cells, or whole cell protein extracts were obtained and the expression of SERCA2a, CSQ, CRT was measured by immunoblotting. **A-D**, Representative traces of caffeine-induced elevations of $[Ca^{2+}]_i$ in H9c2 cells treated with vehicle (A) or ALN in concentrations 10^{-8} M (B), 10^{-7} M (C) and 10^{-6} M (D). Administration of caffeine is indicated by the black bars. Shown are traces from one of three independent experiments. **E**, Compared to vehicle-treated H9c2 cells, the percentage of cells responding to caffeine with transient elevation of $[Ca^{2+}]_i$ was significantly reduced in cultures treated with 10^{-8} M and 10^{-6} M ALN but not 10^{-7} M ALN. Data are means \pm SEM, n = 3-4 independent experiments, different letters indicate significantly different data. **F**, The amplitude of the caffeine induced transients was significantly decreased in H9c2 cells treated with 10^{-8} M ALN compared to vehicle-treated cells. **G**, The spread of the transient, quantified as $t_{down}-t_{response}$ (see Fig. 4E), was significantly reduced in cells treated with 10^{-7} M ALN. For F-G, Data are means \pm SEM, n = 5-16 cells from 3-4 independent experiments. *indicates significant difference compared to vehicle-treated cells. **H**, Long-term treatment of H9c2 cells with ALN differentially affects the expression of SERCA2a, CSQ, and CRT. *Left* - Representative immunoblots from H9c2 cells treated for 48 h with vehicle (Veh), ALN (10^{-6} , 10^{-7} or 10^{-8} M), FTI-277 (10^{-6} M) or GGTI-298 (5^{-6} M) as indicated. *Right* - The expression of SERCA2a, CSQ, CRT were normalized to the expression of GAPDH and presented relative to the levels observed in vehicle-treated cells (indicated by the dashed line). Data are means \pm SEM, n = 3 independent experiments, *indicates significant difference compared to vehicle-treated cells as assessed by t-test.

CHAPTER IV –CONCLUSION AND DISCUSSION

Our data demonstrate that treatment with ALN affects calcium dynamics in atrial cardiomyocytes. We found that ALN induced transitory oscillations of $[Ca^{2+}]_i$, which stabilized within 5 min of treatment. In addition, we found that even short exposure to the highest dose of alendronate affected the timing and amplitude of responses to subsequent application of caffeine. Long term exposure to ALN significantly affected the timing of caffeine-induced calcium responses both in atrial and ventricular cells, and importantly, led to development of oscillations in $[Ca^{2+}]_i$ in atrial cells treated with caffeine. The changes in calcium dynamics were accompanied by significant alterations in expression of SERCA2a, CSQ and CRT. In contrast, alendronate had no effect on farnesylation of HDJ-2 in atrial or ventricular cells, and affected geranylation of RAP-1 only in atrial cardiomyocytes.

Disruption of caffeine-induced calcium signals and appearance of Ca^{2+} oscillations in cells treated with ALN are of particular interest, since abnormalities in calcium dynamics, and specifically development of self-sustained Ca^{2+} oscillations, have been long recognized for their potential contribution to the development of arrhythmias^{30,38,39}. In isolated heart, it has been shown that Ca^{2+} transients can induce and modulate electrical activity^{30,40}, and that spontaneous Ca^{2+} oscillations may lead to ventricular arrhythmia²⁹. Moreover, it has been

shown that large frequent spontaneous Ca^{2+} oscillations distinguish affected heart in dogs that are predisposed to lethal arrhythmia from those in control dogs⁴¹. The potential pacemaker role of Ca^{2+} oscillations is recognized in other tissues exhibiting coordinated behavior, such as smooth muscles of gastrointestinal tract⁴², endocrine cells⁴³ and neurons⁴⁴.

We have found that addition of ALN to atrial cardiomyocytes acutely induced oscillations in $[\text{Ca}^{2+}]_i$. These oscillations were relatively short-lived, but interestingly exhibited ~1.5-fold higher frequency in cells treated with low concentration of ALN compared to higher concentrations. Although $[\text{Ca}^{2+}]_i$ levels stabilized relatively fast following ALN treatment, the subsequent responses of atrial cardiomyocytes to caffeine were affected. Both in cells treated with ALN for 5 min and for 48 h caffeine-induced calcium responses were delayed, and the rate of calcium increase was slowed. Interestingly, after 48 h of treatment with ALN the caffeine-induced calcium elevations exhibited an oscillatory component, which was characterized by frequencies similar to those observed following acute application of alendronate, including the trend for a higher frequency at low concentration of alendronate. These similarities in Ca^{2+} oscillation frequencies observed following treatment with ALN in quite different conditions – one acutely, another in response to caffeine following long-term treatment – I suggest that the role of ALN may be in supporting rather than inducing these oscillatory regimes. The difference in the frequency of Ca^{2+} oscillation in response to treatment with different concentrations of ALN is of potential importance, since it has been

shown before that the Ca^{2+} oscillation frequency may relay information leading to differential regulation of gene expression^{45,46}, Ca^{2+} -calmoduline protein kinase II⁴⁷, and neuronal differentiation⁴⁸.

The concentration-dependence of the ALN actions appears to be quite complex. In atrial cardiomyocytes, we have found that acute treatment with highest concentration of ALN affects responsiveness of HL-1 cells to caffeine as well as the characteristics of caffeine-induced responses, resulting in delayed, slower and smaller transients, whereas cells treated with lower concentrations of ALN appeared to be quite similar to control. In contrast, after 48 h of treatment cells treated with the highest ALN concentrations responded to caffeine most similarly to control, whereas cells treated with lower concentrations of alendronate started to exhibit delayed and slowed responses. One potential interpretation is that in cells treated with ALN for long time it is observed that the interplay of changes directly induced by ALN with those representing compensatory adaptation to initial perturbation induced by ALN. This results in the most complete recovery in cells initially most affected by exposure to the highest concentration of ALN. In ventricular cardiomyocytes ALN concentration-dependence is similarly complex, also suggesting involvement of several processes in the development of the observed phenotype. Interestingly, in ventricular cells the treatment with lower concentrations of ALN also appeared to induce more differences from control than treatment with higher concentrations. However, no calcium oscillations were noted in ALN-treated ventricular cardiomyocytes.

To address the question of potential mediators of ALN-induced alterations in calcium dynamics we assessed the expression of calcium homeostasis proteins, SERCA2a, CSQ and CRT, following treatment with ALN as well as inhibitors of farnesylation and geranylation FTI-277 and GGTI-298. Although farnesyl pyrophosphate synthase is the known molecular target of nitrogen-containing bisphosphonates, including ALN in bone cells, in atrial cardiomyocytes we did not observe any effect of ALN on HDJ-2 farnesylation. The expression of SERCA2a, CSQ and CRT were not affected by treatment with FTI-277 and GGTI-298, even though we detected ALN-mediated reductions in geranylation of RAP-1 in these cells. In ventricular cells, ALN did not affect HDJ-2 farnesylation or RAP-1 geranylation. Although FTI-277 and GGTI-298 affected the expression of SERCA2a and CSQ, those changes were different compared to ALN-induced stimulation of SERCA2a, CSQ and CRT expression. Thus, it is unlikely that effects of ALN on calcium homeostasis are fully mediated through inhibition of protein prenylation.

In atrial cells, 48 h exposure to higher concentration of ALN induced an increase in SERCA2a and a decrease in CSQ, which was accompanied by an increase in CRT. At the lowest concentration of ALN only CRT was increased significantly. It is difficult to interpret if the changes in SERCA2a, CSQ and CRT are the cause of the observed abnormalities in calcium dynamics, or the consequences of effective adaptation and recovery observed in cells treated with the highest

concentration of ALN. Both SERCA2a and CSQ were previously associated with abnormal calcium dynamics and arrhythmias. In humans, mutations in CSQ2 resulting in either a truncated or missense CSQ2 protein are associated with catecholaminergic polymorphic ventricular tachycardia and sudden cardiac death⁴⁹⁻⁵¹. In mice, reductions in CSQ expression increased the predisposition for arrhythmias^{52,53}. Models of atrial fibrillation have also implicated SERCA2a and CSQ in abnormalities of atrial calcium handling after rapid pacing in a canine model of atrial fibrillation⁵⁴⁻⁵⁶. Increased CSQ is also detrimental for the function of heart, since it can lead to depressed contraction and relaxation⁵⁷, as well as altered calcium dynamics and changes in periodicity in rat ventricles⁵⁸. The expression of CRT is also important for the heart function, since CRT deficiency is lethal due to abnormal cardiac development^{59,60}, and CRT over-expression leads to bradycardia, complete heart block and sudden death⁶¹. Thus, SERCA2a, CSQ and CRT may potentially contribute to the ALN-induced abnormalities in calcium homeostasis, however, notably, of these three proteins, only CRT is induced by the exposure of atrial cardiomyocytes to a low concentration of ALN, which most potently affected calcium dynamics.

In summary, our data indicate that following treatment with ALN both atrial and ventricular cardiomyocytes develop abnormalities in calcium dynamics as well as altered expression profile of SERCA2a, CSQ and CRT. However, only atrial cells exhibit self-sustained oscillations of $[Ca^{2+}]_i$ which may indicate an increased potential for the development of atrial fibrillation. Although it may not be possible

to directly link the effects we observed in vitro to higher incidence of serious atrial fibrillations observed in patients taking bisphosphonates, our study is important in demonstrating biological plausibility of this association and the need for further investigations assessing the in vivo effects of bisphosphonates on heart function and calcium dynamics as a likely intermediary.

REFERENCES

- (1) J. M. Lane, A. C. Serota, B. Raphael, *The Orthopedic clinics of North America* **2006**, *37*, 601-609.
- (2) T. M. Zizic, *Am Fam Physician* **2004**, *70*, 1293-1300.
- (3) I. J. Diel, R. Bergner, K. A. Grotz, *The journal of supportive oncology* **2007**, *5*, 475-482.
- (4) D. M. Black, P. D. Delmas, R. Eastell, I. R. Reid, S. Boonen, J. A. Cauley, F. Cosman, P. Lakatos, P. C. Leung, Z. Man, C. Mautalen, P. Mesenbrink, H. Hu, J. Caminis, K. Tong, T. Rosario-Jansen, J. Krasnow, T. F. Hue, D. Sellmeyer, E. F. Eriksen, S. R. Cummings, *N Engl J Med* **2007**, *356*, 1809-1822.
- (5) S. R. Cummings, A. V. Schwartz, D. M. Black, *N Engl J Med* **2007**, *356*, 1895-1896.
- (6) S. R. Heckbert, G. Li, S. R. Cummings, N. L. Smith, B. M. Psaty, *Archives of internal medicine* **2008**, *168*, 826-831.
- (7) S. R. Heckbert, G. Li, S. R. Cummings, N. L. Smith, B. M. Psaty, *Arch. Intern. Med.* **2008**, *168*, 826-831.
- (8) A. Dimension.
- (9) D. B. Kimmel, *Journal of dental research* **2007**, *86*, 1022-1033.
- (10) E. van Beek, E. Pieterman, L. Cohen, C. Lowik, S. Papapoulos, *Biochem Biophys Res Commun* **1999**, *264*, 108-111.
- (11) M. J. Rogers, *Current Pharmaceutical Design* **2003**, *9*, 2643-2658.
- (12) A. A. Reszka, G. A. Rodan, *Mini reviews in medicinal chemistry* **2004**, *4*, 711-719.
- (13) S. P. Luckman, D. E. Hughes, F. P. Coxon, R. Graham, G. Russell, M. J. Rogers, *J Bone Miner Res* **1998**, *13*, 581-589.
- (14) M. Caraglia, D. Santini, M. Marra, B. Vincenzi, G. Tonini, A. Budillon, *Endocrine-related cancer* **2006**, *13*, 7-26.
- (15) R. E. Hewitt, A. Lissina, A. E. Green, E. S. Slay, D. A. Price, A. K. Sewell, *Clinical and experimental immunology* **2005**, *139*, 101-111.
- (16) R. J. Aviles, D. O. Martin, C. Apperson-Hansen, P. L. Houghtaling, P. Rautaharju, R. A. Kronmal, R. P. Tracy, D. R. Van Wagoner, B. M. Psaty, M. S. Lauer, M. K. Chung, *Circulation* **2003**, *108*, 3006-3010.
- (17) .
- (18) M. D. Bootman, D. R. Higazi, S. Coombes, H. L. Roderick, *J. Cell Sci.* **2006**, *119*, 3915-3925.
- (19) S. Arnaudeau, M. Frieden, K. Nakamura, C. Castelbou, M. Michalak, N. Demaurex, *Journal of Biological Chemistry* **2002**, *277*, 46696-46705.
- (20) .
- (21) C. A. Walker, F. G. Spinale, *J. Thorac. Cardiovasc. Surg.* **1999**, *118*, 375-382.
- (22) M. J. B. a. M. D. B. H. Llewelyn Roderick In *Current Biology*, 2003; Vol. 13, pp R425.

- (23) B. C. Knollmann, D. M. Roden, *Nature* **2008**, *451*, 929-936.
- (24) K. F. Frank, L. Mesnard-Rouiller, G. Chu, K. B. Young, W. Zhao, K. Haghighi, Y. Sato, E. G. Kranias, *Basic Res Cardiol* **2001**, *96*, 636-644.
- (25) S. Gyorko, D. Terentyev, *Cardiovasc Res* **2008**, *77*, 245-255.
- (26) .
- (27) H. Kong, P. P. Jones, A. Koop, L. Zhang, H. J. Duff, S. R. W. Chen, *Biochem. J.* **2008**, *414*, 441-452.
- (28) A. D. C. Jeffrey Lazar In *emedicine*, 2007.
- (29) V. Lakireddy, P. Baweja, A. Syed, G. Bub, M. Boutjdir, N. El-Sherif, *Am J Physiol Heart Circ Physiol* **2005**, *288*, H400-407.
- (30) G. Salama, *Heart Rhythm* **2006**, *3*, 67-70.
- (31) W. C. Claycomb, N. A. Lanson, Jr., B. S. Stallworth, D. B. Egeland, J. B. Delcarpio, A. Bahinski, N. J. Izzo, Jr., *Proc Natl Acad Sci U S A* **1998**, *95*, 2979-2984.
- (32) C. Menard, S. Pupier, D. Mornet, M. Kitzmann, J. Nargeot, P. Lory, *J Biol Chem* **1999**, *274*, 29063-29070.
- (33) J. Hescheler, R. Meyer, S. Plant, D. Krautwurst, W. Rosenthal, G. Schultz, *Circ Res* **1991**, *69*, 1476-1486.
- (34) S. V. Komarova, A. Pereverzev, J. W. Shum, S. M. Sims, S. J. Dixon, *Proc Natl Acad Sci U S A* **2005**, *102*, 2643-2648.
- (35) P. Uhlen, *Sci STKE* **2004**, *2004*, pl15.
- (36) P. H. Liang, T. P. Ko, A. H. Wang, *European journal of biochemistry / FEBS* **2002**, *269*, 3339-3354.
- (37) Y. Ogawa, N. Kurebayashi, T. Murayama, *Advances in biophysics* **1999**, *36*, 27-64.
- (38) B. Swynghedauw, B. Chevalier, D. Charlemagne, P. Mansier, F. Carre, *Cardiovasc Res* **1997**, *35*, 6-12.
- (39) J. Liu, P. J. Noble, G. Xiao, M. Abdelrahman, H. Dobrzynski, M. R. Boyett, M. Lei, D. Noble, *Progress in biophysics and molecular biology* **2008**, *96*, 294-304.
- (40) B. R. Choi, F. Burton, G. Salama, *J Physiol* **2002**, *543*, 615-631.
- (41) S. F. Steinberg, S. Alcott, E. Pak, D. Hu, L. Protas, N. S. Moise, R. B. Robinson, M. R. Rosen, *Am J Physiol Heart Circ Physiol* **2002**, *282*, H1181-1188.
- (42) J. D. Huizinga, C. M. Golden, Y. Zhu, E. J. White, *Neurogastroenterol Motil* **2004**, *16 Suppl 1*, 106-111.
- (43) S. S. Stojilkovic, H. Zemkova, F. Van Goor, *Trends in endocrinology and metabolism: TEM* **2005**, *16*, 152-159.
- (44) J. M. Ramirez, A. K. Tryba, F. Pena, *Current opinion in neurobiology* **2004**, *14*, 665-674.
- (45) R. E. Dolmetsch, K. Xu, R. S. Lewis, *Nature* **1998**, *392*, 933-936.
- (46) W. Li, J. Llopis, M. Whitney, G. Zlokarnik, R. Y. Tsien, *Nature* **1998**, *392*, 936-941.
- (47) P. De Koninck, H. Schulman, *Science (New York, N.Y)* **1998**, *279*, 227-230.
- (48) X. Gu, N. C. Spitzer, *Nature* **1995**, *375*, 784-787.
- (49) A. V. Postma, I. Denjoy, T. M. Hoorntje, J. M. Lupoglazoff, A. Da Costa, P. Sebillon, M. M. Mannens, A. A. Wilde, P. Guicheney, *Circ Res* **2002**, *91*, e21-26.

- (50) S. G. Priori, C. Napolitano, M. Memmi, B. Colombi, F. Drago, M. Gasparini, L. DeSimone, F. Coltorti, R. Bloise, R. Keegan, F. E. Cruz Filho, G. Vignati, A. Benatar, A. DeLogu, *Circulation* **2002**, *106*, 69-74.
- (51) H. Lahat, M. Eldar, E. Levy-Nissenbaum, T. Bahan, E. Friedman, A. Khoury, A. Lorber, D. L. Kastner, B. Goldman, E. Pras, *Circulation* **2001**, *103*, 2822-2827.
- (52) B. C. Knollmann, N. Chopra, T. Hlaing, B. Akin, T. Yang, K. Etensohn, B. E. Knollmann, K. D. Horton, N. J. Weissman, I. Holinstat, W. Zhang, D. M. Roden, L. R. Jones, C. Franzini-Armstrong, K. Pfeifer, *J Clin Invest* **2006**, *116*, 2510-2520.
- (53) N. Chopra, P. J. Kannankeril, T. Yang, T. Hlaing, I. Holinstat, K. Etensohn, K. Pfeifer, B. Akin, L. R. Jones, C. Franzini-Armstrong, B. C. Knollmann, *Circ Res* **2007**, *101*, 617-626.
- (54) J. Kneller, H. Sun, N. Leblanc, S. Nattel, *Cardiovasc Res* **2002**, *54*, 416-426.
- (55) J. A. Vest, X. H. Wehrens, S. R. Reiken, S. E. Lehnart, D. Dobrev, P. Chandra, P. Danilo, U. Ravens, M. R. Rosen, A. R. Marks, *Circulation* **2005**, *111*, 2025-2032.
- (56) W. R. Yeh YH, Qi X, Chartier D, Boknik P, Kaab S, Ravens U, Coutu P, Dobrev D, Nattel S. , *CIRCEP* **2008**, *Online 30 April 2008*.
- (57) Y. Sato, D. G. Ferguson, H. Sako, G. W. Dorn, 2nd, V. J. Kadambi, A. Yatani, B. D. Hoit, R. A. Walsh, E. G. Kranias, *J Biol Chem* **1998**, *273*, 28470-28477.
- (58) Z. Kubalova, I. Gyorke, R. Terentyeva, S. Viatchenko-Karpinski, D. Terentyev, S. C. Williams, S. Gyorke, *J Physiol* **2004**, *561*, 515-524.
- (59) N. Mesaeli, K. Nakamura, E. Zvaritch, P. Dickie, E. Dziak, K. H. Krause, M. Opas, D. H. MacLennan, M. Michalak, *J Cell Biol* **1999**, *144*, 857-868.
- (60) F. Rauch, J. Prud'homme, A. Arabian, S. Dedhar, R. St-Arnaud, *Experimental cell research* **2000**, *256*, 105-111.
- (61) K. Nakamura, M. Robertson, G. Liu, P. Dickie, K. Nakamura, J. Q. Guo, H. J. Duff, M. Opas, K. Kavanagh, M. Michalak, *J Clin Invest* **2001**, *107*, 1245-1253.

RESEARCH COMPLIANCE CERTIFICATES



Graduate Student Research Progress Tracking

Form 3

GRADUATE STUDENT RESEARCH PROGRESS REPORT FORM*To be completed by the supervisor and/or supervisory committee* Indicate if this is an INTERIM report (following an unsatisfactory report)Name: Naomi KemenySupervisor: Svetlana KomarovaDegree & Year: M.Sc. 2 year.

Dates of Applicable Time Period:

Department: DentistryFrom: 2007/08 To: 2008/05

Evaluation of Research Progress							
	Comprehensives	Research Plan	Requisite Knowledge	Research Skills	Motivation	Research Accomplishments	Other
Meets Objectives	<input checked="" type="checkbox"/>	<input type="checkbox"/>					
Fails to Meet Objectives	<input type="checkbox"/>						
NA	<input type="checkbox"/>	<input checked="" type="checkbox"/>					

Explanation of above ratings
<ol style="list-style-type: none"> 1. Excellent research productivity. 2. Demonstrated clear understanding of experimental strategies, its strengths and limitations. 3. Great comprehension of the topic, application of research tools. 4. Expand background section during thesis writing

By signing below, all parties acknowledge that the evaluation and progress described above are acceptable. Please note that failure to meet objectives on any two progress reports may be cited as grounds for requiring that a student withdraw from the program of study.

Overall research progress : satisfactory X ; NOT satisfactory _____;Supervisor: Svetlana Komarova Date: 28 May 2008Student: Naomi Kemeny Date: 28 May 2008Chair or Director of Graduate Studies (or delegate): _____ Date: _____
or advisory/ thesis committee member(s) Student did not sign form and does not agree with evaluation (explanation attached)

Paul Tupper, Math & Stats (Suzanne) (LALURA STONE)